ASIAN JOURNAL OF PHARMACEUTICAL AND CLINICAL RESEARCH

INNOVARE ACADEMIC SCIENCES
Knowledge to Innovation

Vol 18, Issue 11, 2025

Online - 2455-3891
Print - 0974-2441

Research Article

COMBINED EFFECT OF *ULVA RETICULATA* AND *GRACILARIA EDULIS* ON CELL VIABILITY, LIPID ACCUMULATION, AND INFLAMMATORY MARKERS IN 3T3-L1 AND RAW 264.7 CELLS

DEVI M[1]*, GEETHA B[2]

[1]Department of Pharmacology, Faculty of Pharmacy, Dr MGR Educational and Research Institute, Chennai, Tamil Nadu, India. [2]Department of Pharmaceutical Chemistry, Faculty of Pharmacy, Dr MGR Educational and Research Institute, Chennai, Tamil Nadu, India.
*Corresponding author: Devi M; Email: devibabu03@gmail.com

Received: 07 July 2025, Revised and Accepted: 17 September 2025

ABSTRACT

Objectives: The objective of the study was to evaluate the cytoprotective, antioxidant, lipid-lowering, glucose uptake-enhancing, and anti-inflammatory activities of *Ulva reticulata* (UR), *Gracilaria edulis* (GE), and their combination (CA). Marine algae are abundant sources of bioactive compounds with therapeutic potential for metabolic and inflammatory disorders. This study reveals the role of marine extracts UR, GE, and their CA in diabetes and its associated inflammatory conditions.

Methods: 3T3-L1 adipocytes and RAW 264.7 macrophages were used to analyze the activity of the extracts based on their role in adipocyte differentiation, lipid metabolism, insulin resistance, and inflammation. The cell lines were exposed to UR, GE, and CA extracts prepared in ethanol: water (7:3, v/v). Cytotoxicity was assessed using 3-(4,5-dimethylthiazol-2-yl)-2,5-diphenyltetrazolium bromide (MTT) assays. Reactive oxygen species levels were measured to evaluate antioxidant activity. Lipid accumulation was analyzed through lipid droplet staining. Glucose uptake was quantified using 2-NBDG assays. Enzyme-linked immunosorbent assay was performed to measure interleukin-6 (IL-6) levels in lipopolysaccharide-stimulated macrophages.

Results: UR showed the highest bio-compatibility and mild proliferative effects, whereas CA displayed the greatest cytotoxicity at the tested concentrations. Antioxidant activity was strongest in UR, followed by GE, while CA exhibited lower scavenging potential. Despite its cytotoxic profile, CA most significantly reduced lipid accumulation and exerted the most pronounced suppression of IL-6 expression, suggesting that its anti-inflammatory efficacy may be linked to mechanisms independent of cell viability. UR, on the other hand, enhanced glucose uptake more effectively than GE and CA.

Conclusion: The hydroalcoholic extracts of UR and GE, individually and in CA, demonstrate distinct and complementary bio-activities that support their potential as natural agents for managing metabolic syndrome. These findings warrant further *in vivo* studies and mechanistic exploration.

Keywords: *Ulva reticulata*, *Gracilaria edulis*, Antioxidant, Anti-inflammatory, Glucose uptake, Lipid accumulation, 3T3-L1, RAW 264.7, Metabolic syndrome, Marine algae, Interleukin-6, Reactive oxygen species.

 DOI: http://dx.doi.org/10.22159/ajpcr.2025v18i11.55949. Journal homepage: https://innovareacademics.in/journals/index.php/ajpcr

INTRODUCTION

Marine-derived bio-active compounds exhibit significant therapeutic potential across a range of diseases due to their diverse pharmacological activities, including antioxidant, anticancer, antiviral, neuroprotective, and anti-inflammatory effects [1]. Algae are emerging as a sustainable and potent source of bio-active pigments such as carotenoids, with significant antioxidant, anti-inflammatory, and therapeutic potential, offering promising applications in health and commercial industries [2]. Thus, algae-derived natural products offer promising multi-targeted therapeutic potential for diabetes management, making them a compelling focus for future anti-diabetic drug development [3,4]. Nevertheless, Seaweeds and their bioactive compounds exhibit promising anti-diabetic effects by inhibiting carbohydrate-hydrolyzing enzymes, modulating inflammatory cytokines, and improving oxidative stress and lipid profiles, warranting further exploration for therapeutic use [5]. Marine brown algae, particularly through phlorotannins, show significant anti-diabetic potential by inhibiting key enzymes involved in glucose metabolism and thereby offer promising natural alternatives for managing type 2 diabetes [6]. The methanolic extract of *Ulva reticulata* (UR), particularly its chloroform fraction (F4), has demonstrated potent antidiabetic activity by inhibiting key carbohydrate-metabolizing enzymes and enhancing insulin secretion, making it a promising natural therapeutic for diabetes management [7]. *Sargassum prismaticum* is also known to exhibit significant antioxidant and cytotoxic properties, particularly in methanolic extracts, highlighting its potential as a novel source for antioxidant drug development [8]. The peptide FDGIP (P13) from *Caulerpa lentillifera* has demonstrated a potent *in silico* and *in vitro* antidiabetic activity by inhibiting key enzymes and transcription factors involved in Type-2 Diabetes, suggesting its potential as a functional food ingredient for T2D management [9]. Similarly, Carotenoids from *Caulerpa racemosa* demonstrated strong potential in modulating type-2 diabetes markers by targeting key proteins such as MAPK3, AKT1, and PPARG, with molecular docking showing superior binding affinities compared to standard drugs [10]. Overall, Marine algae, rich in bioactive compounds [11], offer promising, sustainable, and multi-targeted strategies for diabetes management through mechanisms like enzyme inhibition and antioxidant effects [12]. Nevertheless, seaweeds and their bioactive compounds hold immense potential as nutritional, therapeutic, and industrial agents, offering antioxidant, anti-obesity, anti-diabetic, and anticancer benefits while also serving roles in bio-fertilizers and bio-energy [13]. Cell-based assays using 3T3-L1 adipocytes and RAW 264.7 macrophages are vital tools for evaluating the therapeutic potential of compounds in metabolic disorders. 3T3-L1 adipocytes provide a well-established model to study adipogenesis [13] and glucose metabolism, thereby mimicking key aspects of diabetes [12]. RAW 264.7 macrophages, on the other hand, are widely employed to investigate inflammation-related mechanisms [14]. These models provide mechanistic insights into lipid accumulation and pro-inflammatory signaling, enabling early-stage screening of bio-active compounds for conditions like metabolic syndrome. *Caulerpa okamurae* extract reduced inflammation and improved glucose uptake and

insulin sensitivity in 3T3-L1 adipocytes and RAW 264.7 macrophages, highlighting their potential for treating obesity-related metabolic disorders [14]. Bio-active fractions from the Alaskan brown seaweed *Fucus distichus* significantly inhibited inflammatory gene expression in RAW 264.7 macrophages and reduced lipid accumulation by up to 55% in 3T3-L1 adipocytes, suggesting potent anti-inflammatory and metabolic regulatory effects [15]. UR (a green macroalga) and *Gracilaria edulis* (GE) (a red macroalga) have been traditionally recognized for their nutritional and medicinal value [16,17]. Recent studies suggest that extracts from these algae possess potent antioxidant and anti-inflammatory properties [18]. However, their combined therapeutic potential remains unexplored. Investigating whether these two algae act synergistically or complementarily in modulating oxidative stress, lipid accumulation, glucose uptake, and inflammation may provide valuable insights for developing natural interventions against metabolic disorders. Accordingly, this study aims to evaluate the cytoprotective, antioxidant, lipid-lowering, glucose uptake-enhancing, and anti-inflammatory effects of UR, GE, and their combination (CA) in murine cell line models.

METHODS

Marine algal collection and extraction

Fresh specimens of UR and GE were collected from Mandapam Coast, Rameshwaram, Tamil Nadu, India, during the winter season. The algae were authenticated by a botanist at the Department of Botany, Madras Christian College, Tambaram East, Chennai, Tamil Nadu, India, and voucher specimens were deposited in the herbarium. The samples were thoroughly washed with tap water followed by distilled water to remove salts, sand, and epiphytes. They were then shade-dried at room temperature for 7–10 days and ground into a fine powder using a mechanical grinder. For extraction, 100 g of powdered material was subjected to Soxhlet extraction using Ethanol/Water (70:30) for 24 h. The extracts were filtered and concentrated using a rotary evaporator under reduced pressure at 40°C. The dried extracts were weighed, stored in airtight containers at 4°C, and labeled as UR and GE. A CA extract was prepared by mixing equal proportions (w/w) of UR and GE extracts before experimental use.

Cell culture of 3T3-L1 and RAW 264.7 cells

3T3-L1 Cells (Murine Fibroblast cells) were purchased from NCCS, Pune, and were cultured in liquid medium (Dulbecco's Modified Eagle Medium [DMEM]) supplemented 10% Fetal Bovine Serum (FBS), 100 µg/mL penicillin, and 100 µg/mL streptomycin, and maintained under an atmosphere of 5% CO_2 at 37°C [19]. The cells are free from microbial contamination, which was confirmed by the color, turbidity, pH, and moving objects under the microscope. The cell culture medium was clear, not showing any moving objects under the microscope, no turbidity, and there was no change in pH of the medium.

3-(4,5-dimethylthiazol-2-yl)-2,5-diphenyltetrazolium bromide (MTT) assay

FBS and antibiotic solution were procured from Gibco (USA). Dimethyl sulfoxide (DMSO) and MTT (5 mg/mL) were obtained from Sigma (USA). DMEM, ×1 Phosphate Buffered Saline (PBS), and other reagents were sourced from India. The 96-well tissue culture plates and wash beakers were purchased from Tarsons (India). The test samples CA, GE, and UR were evaluated for *in vitro* cytotoxicity using the 3T3-L1 cell line through the MTT assay. Briefly, cultured 3T3-L1 cells were harvested and pooled into a 15 mL centrifuge tube. Cells were seeded into 96-well tissue culture plates at a density of 1×10^5 cells/ml (200 µL/well) in DMEM supplemented with 10% FBS and 1% antibiotic solution and incubated at 37°C for 24–48 h in a humidified atmosphere containing 5% CO_2. After incubation, the cells were treated with various concentrations of the test samples diluted in serum-free DMEM. Each treatment was carried out in triplicate, and the cells were incubated for an additional 24 h under the same conditions [20,21]. Following treatment, 10 µL of MTT solution (5 mg/mL) was added to each well, and the plate was incubated for another 2–4 h until purple formazan crystals were observed under an inverted microscope. Subsequently, the medium containing MTT (total volume of 220 µL) was carefully aspirated, and the wells were washed with 200 µL of ×1 PBS. To solubilize the formazan crystals, 100 µL of DMSO was added to each well, and the plate was gently shaken for 5 min. The absorbance was measured at 570 nm using a microplate reader (Thermo Fisher Scientific, USA). The percentage of cell viability and IC_{50} values were calculated using GraphPad Prism version 6.0 (USA). For the ROS assay, intracellular reactive oxygen species (ROS) generation was assessed using 2′,7′-dichlorofluorescin diacetate (DCFDA; Sigma, USA) as the fluorescent dye. After the treatment period, cells were incubated with 10 µM DCFDA in serum-free DMEM for 30 min at 37°C in the dark. Following incubation, the wells were washed with ×1 PBS to remove excess dye. Fluorescence intensity was measured at an excitation wavelength of 485 nm and an emission wavelength of 535 nm using a fluorescence microplate reader, indicating ROS levels. To induce oxidative stress as a positive control, hydrogen peroxide (H_2O_2) was used at a final concentration of 100 µM, prepared by appropriate dilution from a 30% (w/v) H_2O_2 stock solution.

ROS assay

The sample was tested for ROS production using 3T3 L1. Briefly, the cultured 3T3 cells were harvested by trypsinization and pooled in a 15 mL tube. Then, the cells were plated at a density of 1×10^6 cells/ml into a 24-well tissue culture plate in a DMEM medium containing 10% FBS and 1% antibiotic solution for 24 h at 37°C [22]. The wells were washed and treated with IC_{50} concentration of UR (116.6 µg/mL), GE (98.01 µg/mL), and CA (90.10 µg/mL) test samples in serum-free DMEM medium and incubated at 37°C for 24 h. After 24 h, 1 mL of ROS assay buffer was added, followed by 100 µL of ×1 ROS assay staining solution, which was added to the wells and mixed gently. Then, the plate was incubated for 60 min in a 37°C incubator with 5% CO_2. After the incubation period, the cells were treated with 100 µM H_2O_2, except for control, and the production of ROS was evaluated immediately using a fluorescence imaging system (ZOE, BIO-RAD).

Lipid droplet assay

DMEM, FBS, and antibiotic solution were obtained from Gibco (USA). DMSO and Oil Red O stain were procured from Sigma (USA). Phosphate-buffered saline (1X PBS) was sourced from Himedia (India). The 96-well tissue culture plates and wash beakers were from Tarsons (India). Oil Red O powder (catalog no. O0625) was purchased from Sigma-Aldrich. A stock solution of Oil Red O was prepared by dissolving 0.2 g of the dye in 40 mL of 2-propanol, yielding a 0.5% (w/v) concentration. This solution was stored at room temperature. For each experiment, a working solution was freshly prepared by diluting the stock solution in a 2:3 ratio with distilled water, resulting in a final concentration of 0.2% Oil Red O in 40% 2-propanol. The working solution was filtered immediately before use. Briefly, 3T3-L1 cells were harvested by trypsinization and pooled in a 15 mL centrifuge tube. The cells were seeded into 24-well tissue culture plates at a density of 1×10^5 cells/ml (200 µL/well) in DMEM supplemented with 10% FBS and 1% antibiotic solution and incubated at 37°C for 24–48 h in a humidified 5% CO_2 atmosphere. After incubation, the wells were washed with sterile PBS and pre-treated with the IC_{50} concentrations of the test samples UR (116.6 µg/mL), GE (98.01 µg/mL), and CA (90.10 µg/mL) prepared in serum-free DMEM [23,24]. Each treatment was performed in triplicate, and the cells were incubated for 24 h under the same conditions. Following treatment, Oil Red O staining was performed. The culture medium was aspirated, and cells were washed once with PBS (0.1 M, pH 7.4). Cells were then fixed with 4% formalin in 0.05 M PBS for 20 min. After fixation, cells were washed with sterile double-distilled water followed by treatment with 60% isopropanol for 2 min. Cells were stained with a filtered 0.35% Oil Red O solution in 60% isopropanol for 10 min at room temperature. Excess stain was removed by washing the cells with sterile double-distilled water. The stained cells were mounted using Dako Paramount aqueous mounting medium, and coverslips were applied. Images were captured under an Olympus light microscope at ×40 magnification. To quantify lipid accumulation, the intracellular Oil

Red O stain was extracted from the cells using isopropanol containing 4% Nonidet P-40, and the optical density of the resulting lysates was measured photometrically at 520 nm.

Enzyme-linked immunosorbent assay (ELISA)

RAW 264.7 cells (murine macrophage cell line) were purchased from NCCS, Pune, and cultured in RPMI-1640 medium supplemented with 10% FBS, 100 µg/mL penicillin, and 100 µg/mL streptomycin. The cells were maintained at 37°C in a humidified incubator with 5% CO_2. Briefly, the cultured RAW 264.7 cells were harvested and pooled into a 15 mL centrifuge tube. The cells were then seeded at a density of 1×10^5 cells/ml per well in a 96-well plate. After cell attachment, they were pre-treated with the IC_{50} concentrations of the test compounds UR (116.6 µg/mL), GE (98.01 µg/mL), and CA (90.10 µg/mL) in serum-free RPMI-1640 medium, followed by stimulation with 100 ng/mL lipopolysaccharide (LPS). The cells were incubated for 24 h at 37°C in a humidified 5% CO_2 atmosphere. After incubation, the culture supernatant was collected by centrifugation at 2500 rpm for 5 min and used to measure interleukin-6 (IL-6) levels. The concentration of the pro-inflammatory cytokine IL-6 was quantified using a sandwich ELISA kit (Invitrogen, USA) according to the manufacturer's instructions. The absorbance was read at 450 nm using a microplate reader (Thermo Fisher Scientific, USA) [25-27].

Glucose uptake activity

DMEM medium, FBS, and antibiotic solution were obtained from Gibco (USA). DMSO, D-Glucose, and HEPES were procured from Sigma (USA). ×1 PBS was from Himedia (India). Tissue culture plates and wash beakers were from Tarson (India). The 3T3-L1 cell line (murine fibroblast cells) was purchased from NCCS, Pune, and cultured in DMEM supplemented with high glucose, 10% FBS, 100 µg/mL penicillin, and 100 µg/mL streptomycin. The cells were maintained at 37°C in a humidified 5% CO_2 atmosphere. To assess glucose uptake activity, cells were seeded in 40 mm Petri plates and cultured until they reached 70–80% confluency. Differentiation was induced by maintaining cells in DMEM with 2% FBS for 4–6 days. The extent of differentiation was confirmed by microscopic observation of multinucleated cells. Differentiated cells were serum-starved overnight before the assay. At the time of the experiment, cells were washed once with HEPES-buffered Krebs-Ringer Phosphate (KRP) solution and incubated in KRP buffer containing 0.1% BSA at 37°C for 30 min. The cells were then treated with the IC_{50} concentrations of test drugs UR (116.6 µg/mL), GE (98.01 µg/mL), and CA (90.10 µg/mL), along with a positive control (100 nM insulin) and negative controls, for 30 min at 37°C. D-glucose solution was added simultaneously to each well and incubated for an additional 30 min at 37°C. Following incubation, glucose uptake was terminated by aspirating the treatment solutions, and cells were washed 3 times with ice-cold KRP buffer. The cells were then lysed with 0.1 M NaOH solution, and aliquots of the cell lysates were used to estimate intracellular glucose levels. Each cell lysate sample (100 µL) was processed using a glucose oxidase-peroxidase enzymatic assay kit following the manufacturer's instructions. The absorbance was measured at 505 nm using a microplate reader (Thermo Fisher Scientific, USA). Results were normalized to total protein content in each sample, quantified using a standard BCA protein assay. Glucose uptake was expressed as a percentage increase over control. Data from three independent experiments were analyzed to determine the enhancement in glucose uptake [28].

Statistical analysis

All experiments were independently performed in triplicate to ensure the reproducibility and reliability of the observed results. Data obtained from these experiments are presented as the mean ± standard deviation, which reflects the central tendency and variability among replicates. For statistical evaluation of the differences between multiple groups, one-way analysis of variance (ANOVA) was employed using GraphPad Prism software version 8.4.3 (GraphPad Software Inc., San Diego, CA, USA). This method assesses whether there are any statistically significant differences among the means of three or more independent groups. To further identify specific group differences, Tukey's multiple comparison *post hoc* test was applied following ANOVA. A $p<0.05$ was considered indicative of statistical significance, implying that the observed differences were unlikely to have occurred by chance alone.

RESULTS

Dose-dependent cytotoxic profiles of plant-derived extracts CA, GE, and UR assessed by MTT assay

The MTT assay results for the three tested plant-derived samples CA, GE, and UR demonstrate a clear dose-dependent effect on cell viability, highlighting distinct cytotoxic profiles for each compound. As the concentration increased from 10 µg/mL to 500 µg/mL, a progressive decline in cell viability was observed, with the most pronounced effects occurring at the highest concentrations tested (Fig. 1). Among the three samples, CA exhibited the strongest cytotoxic response, reducing cell viability to approximately 48.3% at 500 µg/mL. This significant reduction suggests a potent anti-proliferative or cytotoxic nature of CA at elevated doses. In comparison, GE showed moderate cytotoxicity, with cell viability decreasing to around 54.6% at 500 µg/mL, whereas UR displayed the mildest effect, maintaining 66.2% viability at the same concentration. As concentrations decreased, all samples showed a gradual recovery in cell viability, indicating reduced cytotoxicity at lower doses. Interestingly, UR not only preserved higher cell viability across all tested concentrations but also exceeded 100% viability at sub-toxic doses (notably between 10 µg/mL and 40 µg/mL). This suggests a possible proliferative or mitogenic effect, implying that UR might support cell growth or enhance metabolic activity at lower concentrations, an effect often associated with adaptogenic or trophic compounds. In contrast, CA consistently recorded the lowest viability values across the entire concentration range, confirming its strong cytotoxic or anti-proliferative potential. GE's effect was intermediate, showing dose-dependent suppression of viability without the pronounced extremes of either CA or UR. Overall, these findings highlight the differential bioactivities of the three compounds. UR appears to be the least cytotoxic and may even possess cell-supportive properties at low concentrations, suggesting its potential use in regenerative or protective therapeutic contexts. CA, with its strong cytotoxic profile, could be explored for anti-cancer or anti-proliferative applications, whereas GE offers a balanced activity spectrum, making it a candidate for moderate cytotoxic interventions. These contrasting

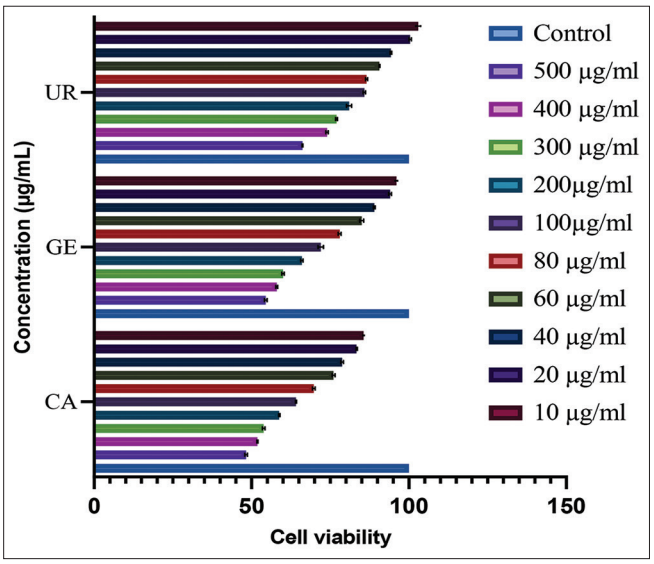

Fig. 1: Effect of different concentrations of tested sample on *Ulva reticulata*, and *Gracilaria edulis*, and combination extract. Data are expressed as mean±Standard deviation. Statistical significance was determined by one-way analysis of variance followed by Tukey's multiple comparison test using GraphPad Prism 8.4.3. $p<0.05$ was considered statistically significant

biological effects emphasize the importance of dose selection and compound specificity when considering their therapeutic utility.

The bar graph displays the percentage of viable cells at each concentration for the respective extracts. The control group, which represents untreated cells, shows 100% viability, serving as the baseline for comparison. A concentration-dependent decrease in cell viability is observed for all extracts, indicating increasing cytotoxicity with higher doses. Among the three extracts, CA exhibits the most pronounced reduction in cell viability, followed by GE and UR, suggesting that CA may possess stronger cytotoxic potential. This data help determine the optimal dose range for further biological evaluation and potential therapeutic applications.

Comparative evaluation of antioxidant activity of UR, GE, and CA using ROS assay

The ROS assay, assessed through fluorescence microscopy, is a critical tool for evaluating intracellular oxidative stress, a key factor implicated in various pathological processes, including neurodegeneration, inflammation, and cancer. In this study, the extent of ROS generation was visualized using a fluorescence-based probe, where increased fluorescence intensity corresponds to elevated ROS levels within the cells (Fig. 2). The control group displayed minimal fluorescence, indicating basal ROS production and a healthy redox balance typical of unstressed cells. This served as a reference for evaluating the oxidative status induced by experimental treatments. Upon exposure to 100 µM/mL of 30% H_2O_2, a potent inducer of oxidative stress, cells exhibited intense green fluorescence, signifying a marked increase in intracellular ROS levels. This confirmed the successful establishment of an oxidative stress model, which is essential for assessing the protective effects of test compounds. Among the treated groups, UR (78.76 µg/mL) showed a substantial reduction in fluorescence intensity compared to the H_2O_2-treated group, indicating a strong ROS-scavenging or antioxidant effect. This suggests that UR effectively mitigates oxidative damage, possibly by enhancing endogenous antioxidant defense systems or directly neutralizing reactive species. Similarly, GE (65.38 µg/mL) demonstrated a moderate reduction in fluorescence, reflecting intermediate antioxidant potential. Although less potent than UR, GE still significantly alleviated oxidative stress, suggesting its beneficial role in redox regulation. In contrast, CA (53.26 µg/mL) exhibited comparatively higher fluorescence, approaching levels observed in the oxidative stress model, thereby indicating a weaker ability to suppress ROS generation. This suggests that CA possesses limited antioxidant activity under the conditions tested, or that its efficacy is dose-dependent and may require higher concentrations for more pronounced effects. In summary, the ROS assay results reveal a clear hierarchy of antioxidant activity among the tested compounds: UR emerged as the most effective ROS scavenger, followed by GE with moderate activity, and CA showing the least effectiveness. These findings underscore the potential of UR and GE as promising candidates for therapeutic applications aimed at counteracting oxidative stress-related cellular damage.

The fluorescence microscopy images illustrate the intracellular ROS levels in cells under various treatment conditions, using a green fluorescent probe to indicate oxidative stress. The control group exhibits minimal fluorescence, suggesting low basal ROS levels in untreated cells. In contrast, cells treated with 100 µM H_2O_2 display intense green fluorescence, confirming the induction of oxidative stress. Cells co-treated with H_2O_2 and plant extracts UR (78.76 µg/mL) and CA (53.26 µg/mL) show significantly reduced fluorescence intensity compared to the H_2O_2-only group, indicating the ROS-scavenging and antioxidant properties of these extracts, as illustrated in Fig. 2. Notably, Cells treated with H_2O_2 alone exhibited intense fluorescence, indicating severe oxidative damage. UR and GE treatments reduced fluorescence to varying extents, while CA treatment most strongly reduced fluorescence to levels comparable with the control, indicating the greatest protection.

Evaluation of lipid-lowering effects of UR, GE, and CA

The lipid droplet assay, visualized through Oil Red O staining, is a widely used histological technique to evaluate intracellular lipid accumulation, which serves as a key indicator of cellular lipid metabolism, storage, and lipogenesis. In this study, the control group exhibited intense staining and was designated as having 100% lipid droplet accumulation, establishing the baseline for comparative analysis. Upon treatment with the test compounds UR, GE, and CA, a marked decrease in lipid droplet staining was observed, suggesting their lipid-lowering potential. Quantitative analysis revealed that UR treatment resulted in a moderate reduction, lowering lipid content to approximately 74.55%, indicating a modest effect on inhibiting lipid buildup. In contrast, GE-treated cells exhibited a more substantial reduction, with lipid droplet accumulation decreasing to 61.82%, reflecting an enhanced modulatory effect on lipid metabolism. The most significant reduction was observed in CA-treated cells, where lipid droplet staining was reduced to 47.79%, demonstrating a robust suppression of intracellular

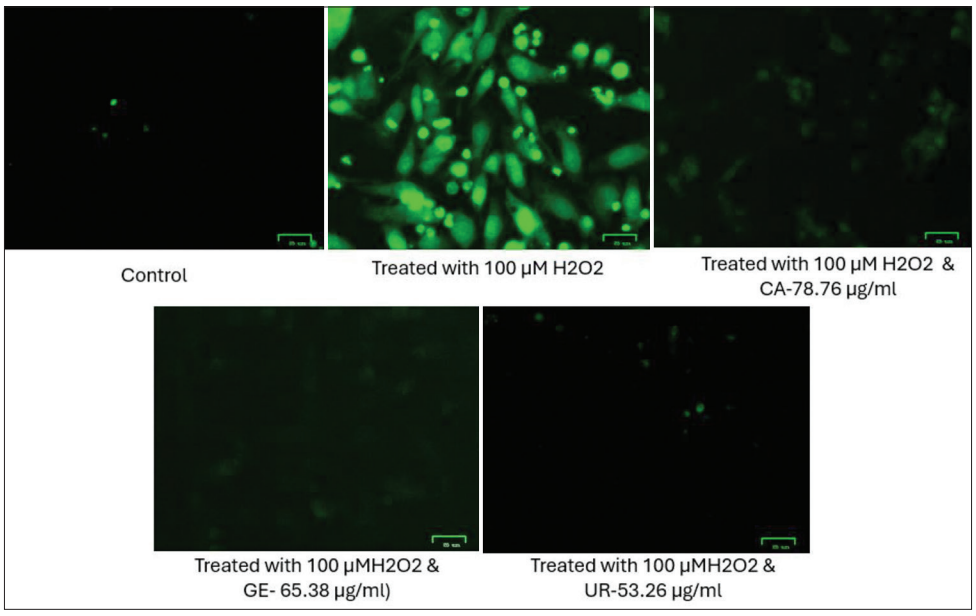

Fig. 2: Protective effect of *Ulva reticulata*, and *Gracilaria edulis*, and combination extract against H_2O_2-induced oxidative stress in SH-SY5Y cells

lipid accumulation, as represented in Fig. 3. This progressive decline in lipid content across UR, GE, and CA treatments suggests a dose-responsive or potency-related trend, with CA emerging as the most effective compound in modulating lipid storage pathways. Collectively, these findings highlight the therapeutic potential of all three extracts in targeting lipid dysregulation, with CA showing the strongest lipid-lowering activity, followed by GE and UR. These results are particularly relevant in the context of metabolic disorders such as obesity, fatty liver disease, and related cardiovascular conditions, where excessive lipid accumulation is a hallmark feature.

The lipid droplet assay images demonstrate the intracellular lipid accumulation in cells treated with different plant extracts, UR, GE, and CA, compared to the untreated control group. Cells were stained using Oil Red O, which specifically binds to neutral lipids and stains lipid droplets red, allowing visualization under a light microscope. The control group shows dense lipid droplet accumulation, indicative of high intracellular lipid content. Treatment with plant extracts resulted in a visible reduction in red staining, especially in GE and CA groups, suggesting a decrease in lipid droplet formation. Among the treatments, CA exhibits the most substantial reduction in lipid accumulation, followed by GE and UR, indicating their potential role in modulating lipid metabolism and exerting anti-lipogenic or lipid-lowering effects. These findings support the therapeutic relevance of these extracts in conditions related to lipid dysregulation.

Comparative analysis of glucose concentration in different extract samples

The glucose uptake assay provides insights into how effectively different compounds stimulate cellular glucose absorption, a key process in energy metabolism and glycemic control. This assay is particularly relevant in identifying therapeutic agents for diabetes, where impaired glucose uptake is a hallmark issue. In this study, the control group cells exposed to glucose alone demonstrated a baseline uptake of 74.13%. When treated with the test compounds, all groups exhibited an increase in glucose absorption, indicating potential glucose-lowering activity. UR (78.76 µg/mL) emerged as the most effective, significantly enhancing glucose uptake to 90.56%. This marked improvement suggests that UR may possess insulin-mimetic or insulin-sensitizing properties, making it a promising candidate for regulating blood glucose levels. CA (53.26 µg/mL) also showed a substantial increase in uptake, reaching 84.62%, further supporting its potential role in promoting glucose utilization. GE (65.38 µg/mL), while still improving glucose absorption compared to the control, had a relatively modest effect with a mean uptake of 76.97%, indicating a mild stimulatory effect on glucose metabolism as represented in Fig. 4. Overall, these findings highlight the differential efficacy of the tested compounds in enhancing glucose uptake. UR demonstrated the most robust activity, followed by CA and then GE. This trend underscores their potential applications in the management of metabolic disorders such as diabetes, with UR standing out as the most promising glucose-regulating agent among the three.

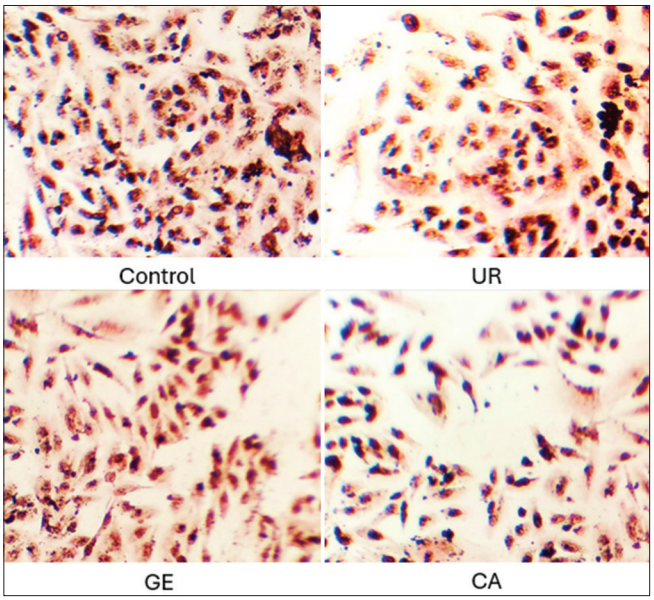

Fig. 3: Visualization of lipid droplet accumulation in treated and control cells using fluorescence microscopy of *Ulva reticulata*, and *Gracilaria edulis*, and combination extract.

This bar graph represents the glucose uptake potential of different treatments, measured in terms of glucose concentration (µg/mL). The black bar (Glucose) denotes the baseline glucose uptake in untreated cells, set at 74.13%. The pink bar (UR) indicates treatment with UR, which significantly increased glucose uptake to 90.56%, demonstrating the strongest stimulatory effect on glucose absorption. The teal bar (GE) represents the GE-treated group, which showed a moderate increase in glucose uptake to 76.97%. The purple bar (CA) reflects the CA-treated group, which elevated glucose uptake to 84.62%, indicating a substantial improvement. This trend illustrates the comparative efficacy of UR, CA, and GE in enhancing glucose metabolism.

Effect of test compounds on LPS-induced IL-6 production in cells by ELISA

The ELISA analysis provided compelling evidence of a pronounced inflammatory response in SH-SY5Y neuroblastoma cells upon LPS stimulation, as indicated by a significant upregulation in IL-6 levels. In untreated control cells, IL-6 concentrations remained within a narrow physiological range of 46.29–47.74 pg/mL, reflecting baseline cytokine expression under normal conditions. However, following LPS exposure, IL-6 production nearly doubled, reaching elevated levels between 96.70 pg/mL and 98.64 pg/ml. This substantial increase clearly confirmed the successful induction of an inflammatory cascade. Importantly, pretreatment of SH-SY5Y cells with test compounds UR, GE, and CA resulted in a notable down-regulation of IL-6 secretion. Specifically, IL-6 concentrations in UR-pretreated cells decreased to approximately 50 pg/mL, while cells treated with GE and CA exhibited IL-6 levels ranging from 47 pg/mL to 48 pg/mL—values that closely mirrored those of the non-inflamed control group which is evidenced from Fig. 5. These findings indicate that UR, GE, and CA possess significant anti-inflammatory properties, as evidenced by their capacity to mitigate LPS-induced cytokine over-expression. Collectively, these results support the potential therapeutic role of these compounds in controlling neuro-inflammation by targeting IL-6-mediated pathways.

The bar graph illustrates the levels of IL-6 expressed in different treatment groups, providing insight into the inflammatory response

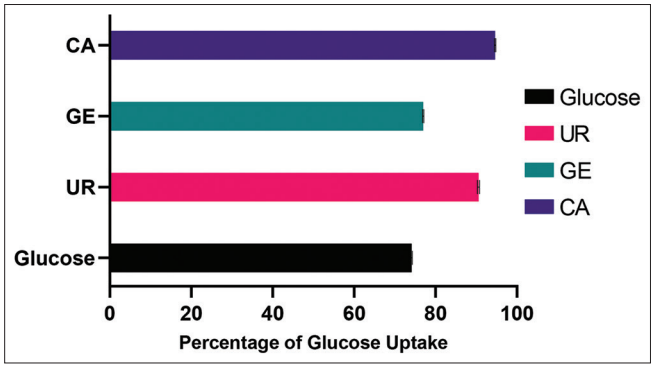

Fig. 4: Percentage of glucose uptake in control (glucose) and extracts of *Ulva reticulata*, and *Gracilaria edulis*, and combination extract. Data are expressed as mean ± standard deviation. Statistical significance was determined by one-way analysis of variance followed by Tukey's multiple comparison test using GraphPad Prism 8.4.3. $p<0.05$ was considered statistically significant

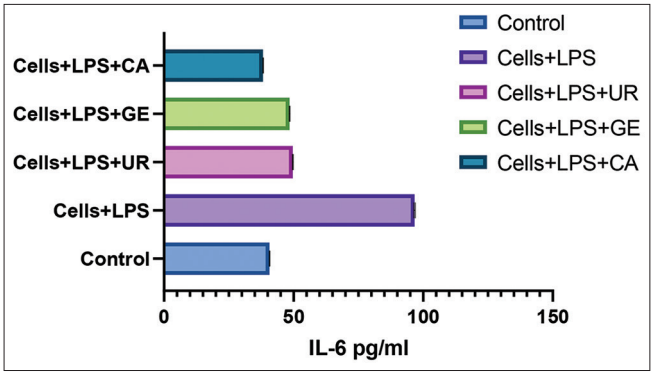

Fig. 5: Effect of *Ulva reticulata*, and *Gracilaria edulis*, and combination extract on lipopolysaccharide-induced interleukin-6 production in cells measured by Enzyme-linked immunosorbent assay. Data are expressed as mean±standard deviation. Statistical significance was determined by one-way analysis of variance followed by Tukey's multiple comparison test using GraphPad Prism 8.4.3. p<0.05 was considered statistically significant

under various conditions. The control group (light blue) exhibited baseline IL-6 levels, representing a normal inflammatory status. When cells were stimulated with LPS alone (purple), IL-6 levels markedly increased, indicating a strong pro-inflammatory response and confirming LPS-induced activation. Co-treatment of LPS-stimulated cells with the test compounds UR (pink), GE (light green), and CA (dark blue) resulted in a noticeable reduction in IL-6 secretion compared to the LPS-only group. Among these, CA showed the most significant suppression, closely followed by GE. Then, UR suggests that all three compounds possess anti-inflammatory properties, with CA being the most potent in attenuating LPS-induced IL-6 production. This trend highlights their potential roles in modulating inflammatory pathways.

DISCUSSION

This study investigates the therapeutic potential of methanolic extracts of UR, GE, and their CA on cellular markers of metabolic dysfunction using 3T3-L1 adipocytes and RAW 264.7 macrophages. The comprehensive evaluation involved assays for cytotoxicity, oxidative stress, lipid accumulation, glucose uptake, and inflammation, key hallmarks of metabolic syndrome and Type 2 diabetes. The data suggest that these marine algae extract hold promise as multi-targeted agents in the management of metabolic disorders. Cytotoxicity screening through the MTT assay revealed distinct viability profiles across the three extracts. CA displayed the strongest cytotoxicity, while UR exhibited the highest bio-compatibility, maintaining >66% viability even at 500 µg/mL. Interestingly, UR promoted slight proliferation at lower concentrations, indicative of possible mitogenic or trophic properties. This aligns with previous reports that certain seaweed constituents may promote cellular health through antioxidant and trophic mechanisms. The mild cytotoxicity of GE and the low toxicity of UR, especially at therapeutic doses, suggest they could be safely employed in long-term or adjunctive therapy for chronic metabolic diseases. Oxidative stress plays a central role in insulin resistance, adipocyte dysfunction, and chronic inflammation. The intracellular ROS assay showed that UR exerted the most robust antioxidant activity, significantly reducing hydrogen peroxide-induced oxidative damage. This may be attributed to its rich content of sulfated polysaccharides, polyphenols, and pigments such as chlorophyll and carotenoids, which scavenge free radicals and enhance endogenous antioxidant defenses. GE also showed moderate antioxidant capacity, while CA's effect was less pronounced, possibly due to interactions among constituents that dampen synergistic antioxidant actions. The strong ROS-scavenging activity of UR and GE supports their role in attenuating oxidative stress-driven metabolic dysfunction. Similarly, *Himanthalia elongata* showed the highest potential among seven commonly consumed seaweeds for managing metabolic syndrome, exhibiting strong antioxidant activity, angiotensin-converting enzyme-I inhibition (IC_{50} = 65 µg/mL), significant reduction of pro-inflammatory markers in LPS-induced RAW 264.7 macrophages, and effective inhibition (43–52%) of triglyceride accumulation in mature 3T3-L1 adipocytes [29]. The Oil Red O lipid accumulation assay demonstrated the extracts' ability to modulate adipogenesis and intracellular lipid storage. CA produced the greatest reduction in lipid droplets, followed by GE and UR. This anti-lipogenic activity may stem from the inhibition of adipogenic transcription factors like PPARγ and C/EBPα or upregulation of lipolytic pathways. The synergistic lipid-lowering effect seen in CA may result from complementary bioactive profiles in UR and GE, enhancing their modulation of lipid metabolism. These findings are promising, considering that excessive adipocyte lipid storage contributes to systemic insulin resistance, inflammation, and obesity. The glucose uptake assay further highlighted UR's standout profile. It significantly enhanced glucose uptake in differentiated 3T3-L1 adipocytes, suggesting insulin-mimetic or insulin-sensitizing effects. This might involve stimulation of the PI3K/Akt signaling pathway, which promotes GLUT4 translocation and glucose absorption. CA also enhanced glucose uptake substantially, while GE showed a modest but significant effect. The superior efficacy of UR supports previous studies reporting its role in enhancing glucose homeostasis, possibly by modulating key regulators such as AMP-activated protein kinase (AMPK) and IRS-1. Enhancing glucose uptake is particularly relevant in diabetes management, where insulin resistance and reduced glucose clearance are critical challenges. The observed activity suggests that these compounds may influence the PI3K/Akt signaling pathway, crucial for GLUT4 translocation and insulin-mediated glucose transport [30]. UR's high efficacy points to its potential in improving insulin sensitivity and glycemic control. Inflammatory cytokines such as IL-6 are central to the chronic inflammation seen in metabolic disorders [31]. Chronic inflammation is a key contributor to metabolic syndrome, with IL-6 serving as a prominent marker of pro-inflammatory responses. ELISA assays revealed that LPS-induced IL-6 expression was markedly attenuated by all three extracts. CA and GE brought IL-6 levels close to those in the unstimulated control group, while UR also demonstrated a significant reduction. This suggests a potent anti-inflammatory effect, possibly through suppression of the NF-κB signaling pathway, which regulates cytokine transcription. The attenuation of IL-6 also suggests potential modulation of TLR4 and MAPK pathways, commonly activated during macrophage-mediated inflammation. Suppression of NF-κB reduces pro-inflammatory gene expression and cytokine release, thereby alleviating insulin resistance and tissue inflammation [32]. These results align with existing literature that seaweed-derived polyphenols, flavonoids, and polysaccharides can inhibit pro-inflammatory cytokine release. Notably, the CA extract CA consistently exhibited synergistic effects in lipid accumulation and inflammation reduction. Although its antioxidant and glucose uptake activities were slightly inferior to UR, the overall multi-targeted efficacy of CA suggests a broad-spectrum therapeutic profile. This synergism likely arises from complementary mechanisms: while UR may predominantly act via oxidative stress and glucose uptake pathways, GE may enhance anti-inflammatory and anti-adipogenic signaling. Such CA therapy could be particularly effective in treating complex metabolic syndromes where multiple pathogenic pathways are involved. These findings are consistent with prior studies where seaweed species such as *C. okamurae* and *F. distichus* demonstrated similar benefits in reducing lipid accumulation, modulating glucose metabolism, and suppressing inflammatory responses in cellular models. Likewise, phlorotannins from brown algae and bioactive peptides from green algae have shown activity against diabetic markers, supporting the growing interest in marine algae as functional therapeutic agents. Nonetheless, the bioactive compounds from *Padina tetrastromatica*, particularly fucoxanthin and lipids, exhibit potent anti-inflammatory effects by modulating cytokine production and reducing pro-inflammatory markers in both 3T3-L1 adipocytes and LPS-induced mouse inflammation models [33]. The ROS-reducing properties of UR and GE suggest activation of the AMPK pathway, a master regulator of energy balance and oxidative stress. AMPK activation has been shown to enhance mitochondrial

function and reduce ROS, thereby preserving insulin sensitivity and metabolic health [34]. The extracts of UR, GE, and CA exhibit distinct yet overlapping bio-activities relevant to the management of metabolic syndrome. UR is notable for its antioxidant and glucose uptake-stimulating effects, GE provides balanced efficacy across all parameters, and CA demonstrates synergistic lipid-lowering and anti-inflammatory properties. These effects likely involve modulation of AMPK, PI3K/Akt, PPARγ, and NF-κB pathways. Given their natural origin, safety profile (especially UR and GE), and pleiotropic effects, these marine extracts hold promise as adjunct therapies in metabolic diseases. Future *in vivo* studies and molecular investigations are warranted to validate their mechanisms and clinical potential.

CONCLUSION

This study elucidates the therapeutic potential of UR, GE, and their CA in modulating key cellular mechanisms associated with metabolic syndrome. UR emerged as a leading candidate due to its low cytotoxicity, potent antioxidant activity, and significant enhancement of glucose uptake. CA demonstrated a synergistic effect, particularly in reducing lipid accumulation and inflammatory cytokine levels, although with higher cytotoxicity. GE exhibited a balanced profile across all parameters. Collectively, these findings suggest that UR and GE, individually or in CA, hold promise as natural interventions for managing oxidative stress, lipid dysregulation, glucose intolerance, and chronic inflammation. Further *in vivo* validation and mechanistic studies are warranted to advance their development as adjunct therapies for metabolic disorders.

ETHICS APPROVAL AND CONSENT TO PARTICIPATE

Not applicable. The study did not involve human participants or animal models.

CONSENT FOR PUBLICATION

Not applicable.

AVAILABILITY OF DATA AND MATERIALS

All data generated or analyzed during this study are included in this published article.

ACKNOWLEDGMENTS

The authors acknowledge the support of the Faculty of Pharmacy, Dr MGR Educational and Research Institute, for providing facilities to conduct the experimental work.

AUTHOR CONTRIBUTIONS

Devi M (First Author): Conceptualization, Methodology, Investigation, Data Curation, Writing – Original Draft.

Devi M (Corresponding Author): Resources, Formal Analysis, Validation, Visualization, Supervision, Project Administration, Writing – Review & Editing. All authors read and approved the final manuscript.

FUNDING

This research received no specific grant from any funding agency in the public, commercial, or not-for-profit sectors.

COMPETING INTERESTS

The authors declare that they have no known competing financial interests or personal relationships that could have appeared to influence the work reported in this paper.

REFERENCES

1. Karthikeyan A, Joseph A, Nair BG. Promising bioactive compounds from the marine environment and their potential effects on various diseases. J Genet Eng Biotechnol. 2022;20(1):14. doi: 10.1186/s43141-021-00290-4, PMID 35080679
2. Patel AK, Albarico FP, Perumal PK, Vadrale AP, Nian CT, Chau HT, *et al*. Algae as an emerging source of bioactive pigments. Bioresour Technol. 2022;351:126910. doi: 10.1016/j.biortech.2022.126910, PMID 35231601
3. Pereira L, Valado A. Algae-derived natural products in diabetes and its complications-current advances and future prospects. Life (Basel). 2023;13(9):1831. doi: 10.3390/life13091831, PMID 37763235
4. Raja E F, Paul J JP. Gas chromatography-mass spectroscopy analysis and prediction of bioactivities in the chloroform extract of *Halymenia dilatata Zanardini* (red algae) collected from Mandapam, Tamil Nadu, India. Asian J Pharm Clin Res. 2021;14:60-3. doi: 10.22159/ajpcr.2021.v14i12.43068
5. Agarwal S, Singh V, Chauhan K. Antidiabetic potential of seaweed and their bioactive compounds: A review of developments in last decade. Crit Rev Food Sci Nutr. 2023;63(22):5739-70. doi: 10.1080/10408398.2021.2024130, PMID 35048763
6. Gunathilaka TL, Samarakoon K, Ranasinghe P, Peiris LD. Antidiabetic potential of marine brown algae-a mini review. J Diabetes Res. 2020;2020:1230218. doi: 10.1155/2020/1230218
7. Unnikrishnan PS, Animish A, Madhumitha G, Suthindhiran K, Jayasri MA, Unnikrishnan PS, *et al*. Bioactivity guided study for the isolation and identification of antidiabetic compounds from edible seaweed- *Ulva reticulata*. Molecules. 2022;27(24):8827. doi: 10.3390/molecules27248827, PMID 36557959
8. Pal S, Soni A, Patel N, Sharma P, Siddiqi NJ, Fatima S, *et al*. Phytochemical profiling, antioxidant potential and cytotoxic activity of *Sargassum prismaticum* extracts: Implications for therapeutic applications. Nat Prod Res. 2024;39:4688-94. doi: 10.1080/14786419.2024.2344745
9. Kurniawan R, Taslim NA, Hardinsyah H, Syauki AY, Idris I, Aman AM, *et al*. Pharmacoinformatics and cellular studies of algal peptides as functional molecules to modulate type-2 diabetes markers. Futur Foods. 2024;9:100354. doi: 10.1016/j.fufo.2024.100354
10. Kurniawan R, Taslim NA, Aman AM, Syauki AY, Bukhari A, Bahar B, *et al*. Pharmacoinformatics and *ex vivo* studies of carotenoids from green algae *Caulerpa racemosa* as functional biomolecules to modulate type-2 diabetes markers. S Afr J Bot. 2025;178:348-59. doi: 10.1016/j.sajb.2025.01.048
11. Gomathi K, Anna Sheba L. Phytochemical screening and heavy metal analysis of *Ulva reticulata*. Asian J Pharm Clin Res. 2018;11(4):84. doi: 10.22159/ajpcr.2018.v11i4.23012
12. Animish A, Jayasri MA, Animish A, Jayasri MA, Animish A, Jayasri MA. A retrospective review of marine algae and the strategies employed for prospective diabetes management. Algal Res. 2023;74:103209. doi: 10.1016/j.algal.2023.103209
13. Pradhan B, Bhuyan PP, Patra S, Nayak R, Behera PK, Behera C, *et al*. Beneficial effects of seaweeds and seaweed-derived bioactive compounds: Current evidence and future prospective. Biocatal Agric Biotechnol. 2022;39:102242. doi: 10.1016/j.bcab.2021.102242
14. Manandhar B, Kim HJ, Rhyu DY, Manandhar B, Kim HJ, Rhyu DY, *et al*. *Caulerpa okamurae* extract attenuates inflammatory interaction, regulates glucose metabolism and increases insulin sensitivity in 3T3-L1 adipocytes and RAW 264.7 macrophages. J Integr Med. 2020;18(3):253-64. doi: 10.1016/j.joim.2020.02.001, PMID 32088151
15. Kellogg J, Esposito D, Grace MH, Komarnytsky S, Lila MA, Kellogg J, *et al*. Alaskan seaweeds lower inflammation in RAW 264.7 macrophages and decrease lipid accumulation in 3T3-L1 adipocytes. J Funct Foods. 2015;15:396-407. doi: 10.1016/j.jff.2015.03.049
16. Djoh EF, Meiyasa F, Ndahawali S, Tarigan N, Djoh EF, Meiyasa F, *et al*. Chemical composition, antimicrobial, and antioxidant activity of *Ulva reticulata* seaweed extracted with different solvents. Biodivers J Biol Divers. 2024;25(9):2943-9. doi: 10.13057/biodiv/d250914
17. Hofmann LC, Strauss S, Shpigel M, Guttman L, Stengel DB, Rebours C, *et al*. The green seaweed *Ulva*: Tomorrow's "wheat of the sea" in foods, feeds, nutrition, and biomaterials. Crit Rev Food Sci Nutr. 2024;65:3728-63. doi: 10.1080/10408398.2024.2370489
18. Reka P, Thahira Banu A, Seethalakshmi M. Alpha amylase and alpha glucosidase inhibition activity of selected edible seaweeds from South Coast area of India. Int J Pharm Pharm Sci. 2017;9(6):64-8. doi: 10.22159/ijpps.2017v9i6.17684
19. Shijina BN, Radhika A, Sherin S, Biju PG. Vindoline exhibits anti-diabetic potential in insulin-resistant 3T3-L1 adipocytes and L6 skeletal myoblasts. Nutrients. 2023;15(13):2865. doi: 10.3390/nu15132865, PMID 37447192
20. Ebrahimi Z, Irani S, Ardeshirylajimi A, Seyedjafari E. Enhanced osteogenic differentiation of stem cells by 3D printed PCL scaffolds coated with collagen and hydroxyapatite. Sci Rep. 2022;12(1):12359.

doi: 10.1038/s41598-022-15602-y, PMID 35859093

21. Cho YJ, Lee JB, Lee Y, Lee MS, Choi J. Inhibition of differentiation of 3T3-L1 cells by increasing glioma-associated oncogene expression in *Chrysanthemum indicum* L. Using *Lactococcus lactis* KCTC 3115. Prev Nutr Food Sci. 2024;29(4):533-45. doi: 10.3746/pnf.2024.29.4.533, PMID 39759806
22. Lee H, Lee YJ, Choi H, Ko EH, Kim JW. Reactive oxygen species facilitate adipocyte differentiation by accelerating mitotic clonal expansion. J Biol Chem. 2009;284(16):10601-9. doi: 10.1074/jbc.M808742200
23. Rath S, Maiti D, Modi M, Pal P, Munan S, Mohanty B, *et al*. Metal-free synthesis and study of glycine betaine derivatives in water for antimicrobial and anticancer applications. iScience. 2023;26(8):107285. doi: 10.1016/j.isci.2023.107285, PMID 37575199
24. Kaczmarek I, Suchý T, Strnadová M, Thor D. Qualitative and quantitative analysis of lipid droplets in mature 3T3-L1 adipocytes using oil red O. Star Protoc. 2024;5(2):102977. doi: 10.1016/j.xpro.2024.102977, PMID 38875117
25. Sudeep HV, Gouthamchandra K, Ramanaiah I, Raj A, Naveen P, Shyamprasad K. A standardized extract of *Echinacea purpurea* containing higher chicoric acid content enhances immune function in murine macrophages and cyclophosphamide-induced immunosuppression mice. Pharm Biol. 2023;61(1):1211-21. doi: 10.1080/13880209.2023.2244000, PMID 37585723
26. Oh YJ, Jin SE, Shin HK, Ha H. Daeshiho-tang attenuates inflammatory response and oxidative stress in LPS-stimulated macrophages by regulating TLR4/MyD88, NF-κB, MAPK, and Nrf2/HO-1 pathways. Sci Rep. 2023;13(1):18891. doi: 10.1038/s41598-023-46033-y, PMID 37919391
27. Jeong GH, Lee H, Woo SY, Lee HK, Chung BY, Bai HW. Novel aminopyridazine derivative of minaprine modified by radiolysis presents potent anti-inflammatory effects in LPS-stimulated RAW 264.7 and DH82 macrophage cells. Sci Rep. 2023;13(1):10887. doi: 10.1038/s41598-023-37812-8, PMID 37407652
28. Takigawa-Imamura H, Sekine T, Murata M, Takayama K, Nakazawa K, Nakagawa J. Stimulation of glucose uptake in muscle cells by prolonged treatment with Scriptide, a histone deacetylase inhibitor. Biosci Biotechnol Biochem. 2003;67(7):1499-506. doi: 10.1271/bbb.67.1499, PMID 12913293
29. Rico D, Diana AB, Milton-Laskibar I, Fernández-Quintela A, Silván JM, Rai DK, *et al*. Characterization and *in vitro* evaluation of seaweed species as potential functional ingredients to ameliorate metabolic syndrome. J Funct Foods. 2018;46:185-94. doi: 10.1016/j.jff.2018.05.010
30. Zhu Y, Pereira RO, O'Neill BT, Riehle C, Ilkun O, Wende AR, *et al*. Cardiac PI3K-Akt impairs insulin-stimulated glucose uptake independent of mTORC1 and GLUT4 translocation. Mol Endocrinol. 2013;27(1):172-84. doi: 10.1210/me.2012-1210, PMID 23204326
31. Hirano T. IL-6 in inflammation, autoimmunity and cancer. Int Immunol. 2021;33(3):127-48. doi: 10.1093/intimm/dxaa078, PMID 33337480
32. Liu T, Zhang L, Joo D, Sun SC. NF-κB signaling in inflammation. Signal Transduct Target Ther. 2017;2(1):17023. doi: 10.1038/sigtrans.2017.23, PMID 29158945
33. Sharma PP, Chonche MJ, Mudhol S, Muthukumar SP, Baskaran V. Anti-inflammatory efficacy of brown seaweed (*Padina tetrastromatica*) in 3T3-L1 adipocytes and low-dose LPS induced inflammation in C57BL6 mice. Algal Res. 2023;71:103027. doi: 10.1016/j.algal.2023.103027
34. Hinchy EC, Gruszczyk AV, Willows R, Navaratnam N, Hall AR, Bates G, *et al*. Mitochondria-derived ROS activate AMP-activated protein kinase (AMPK) indirectly. J Biol Chem. 2018;293(44):17208-17. doi: 10.1074/jbc.RA118.002579, PMID 30232152